Quantum Electronics **37** (6) 565 – 574 (2007)

INTERACTION OF LASER RADIATION WITH MATTER

PACS numbers: 78.20. – e; 78.20.Ci; 36.40. – c; 36.40.Gk; 36.40.Vz
DOI: 10.1070/QE2007v037n06ABEH013428

Collisionless absorption of intense laser radiation in nanoplasma

D.F. Zaretsky, Ph.A. Korneev, S.V. Popruzhenko

Abstract. **The rate of linear collisionless absorption of an electromagnetic radiation in a nanoplasma – classical electron gas localised in a heated ionised nanosystem (thin film or cluster) irradiated by an intense femtosecond laser pulse – is calculated. The absorption is caused by the inelastic electron scattering from the self-consistent potential of the system in the presence of a laser field. The effect proves to be appreciable because of a small size of the systems. General expressions are obtained for the absorption rate as a function of the parameters of the single-particle self-consistent potential and electron distribution function in the regime linear in field. For the simplest cases, where the self-consistent field is created by an infinitely deep well or an infinite charged plane, closed analytic expressions are obtained for the absorption rate. Estimates presented in the paper demonstrate that, over a wide range of the parameters of laser pulses and nanostructures, the collisionless mechanism of heating electron subsystem can be dominant. The possibility of experimental observation of the collisionless absorption of intense laser radiation in nanoplasma is also discussed.**

Keywords: *nanoplasma, collisionless absorption.*

1. Introduction

The development of high-power femtosecond lasers over the past 10 – 15 years has stimulated new experimental studies of the interaction of various nanosystems with an intense electromagnetic radiation. As nanosystems, metal or atomic clusters of diameter from a few to hundreds of nanometers are widely used which contain from several tens to tens of millions of atoms (see reviews [1 – 3]). Thin films are also used in experiments, though rarely than clusters [4]. Short laser pulses with intensities of $10^{14} - 10^{21}$ W cm^{-2} induce internal ionisation in nanosystems to form a plasma with the mean electron energy from tens to tens of thousands of electron-volts. A part of electrons escape from the system (external ionisation), producing an uncompensated charge that traps the rest of the plasma, which then evolves within a finite volume until the decay of the ion core of a nanobody. The characteristic expansion time of the electron subsystem is hundreds of femtoseconds and more [see estimate (2) below]. Thus, a new physical object appears on the femtosecond time scale – a dense hot electron plasma localised on a nanometer spatial scale, the so-called nanoplasma [5, 6]. At present, physical properties of nanoplasmas are being extensively studied both theoretically and experimentally.

A high absorptivity in the optical and IR ranges is one of the most important properties of nanoplasmas in a strong laser field. It has been shown experimentally that nanoplasma absorbs laser radiation much more efficiently (per atom) than gaseous target, macroplasma, or a solid [5]. The efficient absorption of laser radiation leads to fast heating of the electron subsystem, and as a result, the nanoplasma becomes a source of high harmonics, characteristic X-rays, and fast-ion and multicharged-ion emission. At present, these effects and their possible practical applications are being extensively studied (see papers [2 – 4] and references therein).

The high absorptivity of a nanoplasma observed in an intense laser field was interpreted by using several different mechanisms such as the inverse multiphoton retardation effect [5 – 7], vacuum heating [8, 9], stochastic heating [10], etc. In this work, we consider a collisionless absorption mechanism based on the electron interaction with the self-consistent field of a nanostructure in the presence of the alternating electric field of the laser wave. The collisionless absorption effect was first considered by Landau in 1946. He showed that the longitudinal electromagnetic waves propagating in an infinite plasma can be damped without collisions [11, 12] (Landau damping). As a rule, the collisionless absorption occurs through the so-called resonance particles. In the case of linear Landau damping in an infinite plasma, the resonance condition has the form [11, 12]

$$\boldsymbol{k}\boldsymbol{v} = \omega, \tag{1}$$

where ω и $\boldsymbol{k}$ are, respectively, the frequency and wave vector of the longitudinal wave, and $\boldsymbol{v}$ is the electron velocity. These particles move in phase with the wave and can receive from or impart to it nonzero time-averaged energy. In a finite-size plasma, the collisionless absorption acquires qualitatively new features, which were first examined in [13] for a homogeneous layer of a classical (nondegenerate) plasma and in [14] for small cold spherical metal particles. The main qualitative result is that the

D.F. Zaretsky Russian Research Center 'Kurchatov Institute', pl. akad. Kurchatova 1, 123182 Moscow, Russia;
Ph.A. Korneev, S.V. Popruzhenko Moscow Engineering Physics Institute (State University), Kashirskoe shosse 31, 115409 Moscow, Russia;
e-mail: korneev@theor.mephi.ru

Received 13 September 2006
Kvantovaya Elektronika **37** (6) 565 – 574 (2007)
Translated by V.P. Sakun

collisionless absorption mechanism can dominate due to the intense electron interaction with the system boundary. The electron collision with boundary is nothing but its interaction with a self-consistent potential. To avoid confusion, we emphasise that by a collisionless absorption is meant the absence of pair collisions or their insignificance, whereas the collisions with boundary are significant; roughly speaking, they are the physical reason for the effect.

Recently, the collisionless energy absorption in laser-heated clusters and thin films has become the subject of extensive theoretical studies [15–22]. In particular, it has been shown that the width of the Mie resonance in clusters can be determined by the frequency of electron collisions with the cluster boundary rather than by the electron–ion collision frequency. In [15], the collisionless absorption rate was calculated for the limiting case of a very high laser-field intensity, when the amplitude of electron-cloud oscillations exceeds the cluster radius. In this case, the interaction with the ion core can be taken into account in the first Born approximation, whereas the interaction with the laser field can be treated exactly. The absorption proves to be essentially nonlinear in field and strong enough, because each electron is scattered by the whole ion core rather than by individual ions.

Another limiting case corresponding to relatively weak fields, for which the amplitude of electron-cloud oscillations is small compared to the system size, so that the absorption regime is linear, was considered in [17] and [18] for thin films and spherical clusters, respectively. This regime occurs in a wide range of parameters, so that even the radiation of intensity 10^{17} W cm^{-2} can be weak for the systems tens of nanometers in size. A similar problem of the collisionless damping of an electromagnetic wave in a hot homogeneous plasma layer was solved in [19] for one of the limiting cases where the frequency of electron collisions with layer boundaries is small compared to the laser frequency. For the case where the self-consistent field modeling plasma can be approximated by the potential of an infinitely deep rectangular well, closed expressions for the energy absorption rate and the imaginary part of the dielectric constant were obtained in [17–19].

Finally, the collisionless energy absorption was studied in [20–22] by using the model of a nonlinear oscillator describing laser-induced oscillations of an incompressible electron cloud. It was shown that the absorption becomes strong when the amplitude-dependent Mie frequency becomes close to the laser frequency. The conclusions drawn in these works are in qualitative agreement with the results of numerical computations carried out in [22].

The estimates based on the analytic expressions [13, 17–19] and the numerical results obtained in [22] indicate that the Landau damping can play an important role in plasma heating and even dominate it for the femtosecond laser pulses with intensities of $10^{14} - 10^{16}$ W cm^{-2} and thin films (clusters) of size less than 100 nm.

In this work, the theory formulated in [17, 18] is developed. The linear collisionless absorption rate in a classical nanoplasma representing one-dimensional (film) and three-dimensional (spherical cluster) systems is calculated and studied as a function of the shape of the self-consistent potential and the form of the electron distribution function. The results, in particular, can be used to discuss the experimental manifestations of the collisionless absorption effect.

2. Statement of the problem

The electron plasma is produced in a nanostructure due to internal ionisation at the laser pulse front. Due to the energy absorption, plasma is heated and a part of electrons escape from the system (external ionisation). For not too small clusters (thin films) of size $a \simeq 10$ nm and not too strong radiation fields with intensity $I \simeq 10^{14}$–10^{16} W cm^{-2}, most of the electrons remain trapped and form a nanoplasma, which exists, at least, for hundreds of femtoseconds, until the system decays due to the Coulomb explosion [23]. Ions and trapped electrons form the self-consistent potential having the oscillating component in the laser field. If the core of the system is formed by ions of mass m_i and average charge $\overline{Z}_i$, the characteristic expansion time of ions is [24]

$$\tau_i \sim \left(\frac{m_i}{e^2 n_{tr} \overline{Z}_i \eta}\right)^{1/2}, \qquad (2)$$

where e is the elementary charge; $n_{tr} = n_i \overline{Z}(1-\eta)$ is the average concentration of trapped electrons; η is the degree of external ionisation of the system; and n_i is the ion concentration. For a cluster consisting of xenon atoms, for $n_{tr} \simeq 5 \times 10^{22}$ cm^{-3}, $\overline{Z}_i = 4$, $\eta \approx 0.1$, estimate (2) gives $\tau_i \approx 300$ fs. Therefore, on the time scale of tens of femtoseconds, the plasma trapped in a film or a cluster can be treated as stationary with the time-independent electron concentration $n_e^0(\boldsymbol{r})$. Strictly speaking, the function $n_e^0(\boldsymbol{r})$ should be found by solving simultaneously the Boltzmann equation for the distribution function and the Poisson equation for the electric potential. In this work, we do not consider this problem, assuming that the self-consisted potential and concentration are known functions. Note that the time τ_i (2) weakly depends on the cluster size (the size dependence enters through the degree η of external ionisation; for small clusters, it is higher, all factors being the same). The dependence of τ_i (2) on the mass m_i of plasma ions makes the stationary-nanoplasma approximation inapplicable to light clusters (D_2, D_2O), whereas the same approximation applies nicely to heavy elements (Ar, Xe, metal clusters) up to hundreds of femtoseconds.

Laser field excites various vibrational modes of a nanoplasma. For small spherical bodies ($a \ll \lambda$, where λ is the laser radiation wavelength), these modes were found in [19] for the case that the plasma oscillations can be described in the hydrodynamic approximation. However, the hydrodynamic description, in general, does not apply to the problem considered, because it is valid under the condition $a \gg l_0$, where l_0 is the mean free path*. In nanostructures subjected to the intense laser field, the ratio between the system size and the mean free path is often reverse. We assume here that the electron cloud executes small-amplitude oscillations without deformation, i.e., that only a surface plasmon is excited. The necessary condition for the incompressible-liquid approximation to properly describe the electron-cloud oscillations is that the amplitude ξ_0 of these oscillations should be small compared to the system size: $\xi_0 \ll a$. Moreover, one of the two additional requirements is to be met: either a relative change in the

*Strictly speaking, the hydrodynamic equations can apply to plasma in the opposite limit $a \ll l_0$ [25] as well. However, this requires fulfillment of some additional conditions that strongly narrows the range of laser field and nanoplasma parameters.

equilibrium electron density inside the system be small, or the laser frequency ω be large enough: $\omega \gg \omega_{pD}$, where $\omega_{pD} = [4\pi \overline{Z} n_i e^2 \kappa/(D m_e)]^{1/2}$ is the plasmon frequency depending on the dimensionality D of a nanostructure; κ is the fraction of electrons trapped in the ion core; and m_e is electron mass. In the latter case, the electric field inside the system is little different from the external laser field and, hence is almost uniform.

Note that the high-frequency limit is of particular interest in studying the nanoplasma interaction with intense electromagnetic radiation. For instance, upon the interaction of thin semiconductor films with the optical or IR laser radiation of intensity $10^{13} - 10^{14}$ W cm^{-2}, the initially empty conduction band is gradually filled with electrons due to multiphoton absorption. In this case, plasma heating in the conduction band occurs under the condition $\omega \gg \omega_{pD}$, and the film fails upon reaching resonance [26]. Furthermore, free electron lasers were recently used to fabricate coherent radiation sources with a photon energy of 10–15 eV and intensity up to 10^{13} W cm^{-2}. The experiments performed with these sources on the interaction of such fields with clusters [27, 28] revealed an anomalously strong UV absorption. Obviously, the condition is also met for photons with energies 10–15 eV.

Under the action of an external linearly polarised laser field of strength

$$\boldsymbol{E}(t) = \boldsymbol{E}_0 \cos(\omega t + \alpha) \tag{3}$$

the electron cloud oscillates with the amplitude

$$\xi_0 = \frac{eE_0}{m_e\left[(\omega^2 - \omega_{pD}^2)^2 + 4\Gamma^2\omega^2\right]^{1/2}}. \tag{4}$$

The resonance width Γ is caused by various relaxation processes, including the collisionless Landau damping. Beyond the resonance, $|\omega - \omega_{pD}| \gg 1$, amplitude (4) is ordinarily small compared to the system size a. As an example, we consider a cluster ($D = 3$) with radius $a \simeq 10$ nm and mean electron concentration $\overline{n}_e \simeq \overline{Z}_i n_i \simeq 10^{23}$ cm^{-3}. The relevant energy of the surface plasmon (Mie resonance) is $\hbar\omega_{p3} \equiv \hbar\omega_{Mie} \approx 6$ eV, so that the linear resonance is not achieved for the radiation from a Ti : sapphire laser with frequency $\omega = 1.55$ eV. Expression (4) gives $\xi_0 \simeq 1$ nm, i.e., a value an order of magnitude smaller than the radius even for the radiation with intensity $I = 5 \times 10^{16}$ W cm^{-2}. This estimate demonstrates that, beyond the resonance, the approximation linear in the external field adequately describes the electron-cloud oscillations even for high field intensities. Near the resonance, this approximation can become inadequate. Below, we assume that the condition $\xi_0 \ll a$ is fulfilled.

The laser-energy absorption rate $\overline{Q}$ is equal to the time-averaged work executed on electrons by the internal electric field. The variable field component inside the nanoplasma is the sum of the laser and induced fields. In the linear and dipolar approximations, the relation between the internal and applied fields can be found with ease. We illustrate this by the example of a one-dimensional system (film) in the field of linearly polarised laser radiation (3). In the approximation of an incompressible electron cloud, its displacement $\xi_0 \ll a$ in the direction perpendicular to the film plane obeys, under the condition $\xi(t)$, the equation of a harmonic oscillator

$$\ddot{\xi} + 2\Gamma_1\dot{\xi} + \omega_{p1}^2\xi = -\frac{eE_{0z}}{m_e}\cos(\omega t + \alpha). \tag{5}$$

The angles specifying the polarisation and field-propagation directions are shown in Fig. 1. The solution to Eqn (1) has the form

$$\xi(t) = -\frac{eE_{0z}}{m_e\left[(\omega^2 - \omega_{p1}^2)^2 + 4\Gamma_1^2\omega^2\right]^{1/2}}\cos(\omega t + \alpha + \beta),$$
$$\sin\beta = -\frac{2\Gamma_1\omega}{\left[(\omega^2 - \omega_{p1}^2)^2 + 4\Gamma_1^2\omega^2\right]^{1/2}}. \tag{6}$$

Assuming that the electron distribution in the film is close to uniform and the damping is small ($\Gamma_1 \ll \omega,\ \omega_{p1}$), we obtain the expression for the internal-field strength:

$$\mathcal{E}(t) = 4\pi e\overline{n}_e\xi(t)\boldsymbol{e}_z + \boldsymbol{E}_0\cos(\omega t + \alpha)$$
$$= \boldsymbol{\mathcal{E}}_{0\perp}\cos(\omega t + \alpha) + \boldsymbol{e}_z\mathcal{E}_z\cos(\omega t + \alpha - \delta),$$
$$\boldsymbol{\mathcal{E}}_{0\perp} = \boldsymbol{E}_{0\perp}, \quad \mathcal{E}_z = \frac{E_{0z}}{\left[(1 - \omega_{p1}^2/\omega^2)2 + 4\Gamma_1^2/\omega^2\right]^{1/2}}, \tag{7}$$

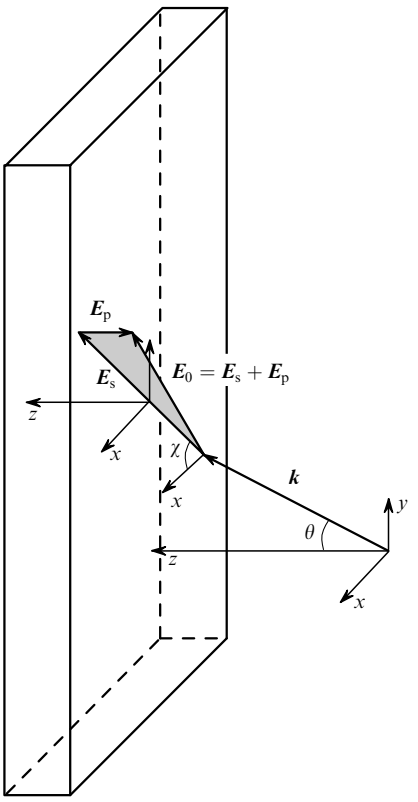

Figure 1. Geometry of the problem for a one-dimensional system (film). The external (laser) field is directed along the wave vector $\boldsymbol{k}$ at the angle θ to the z axis perpendicular to the film. The electric vector $\boldsymbol{E}_0$ is directed at the angle χ to the x axis; $\boldsymbol{E}_s$ is the $\boldsymbol{E}_0$ component in the film plane xy, and $\boldsymbol{E}_p$ is the $\boldsymbol{E}_0$ component parallel to the z axis.

$$\sin\delta = \left(\frac{\omega_{\rm p1}}{\omega}\right)^2 \sin\beta,$$

where $\boldsymbol{e}_z$ is the unit vector along the z axis. The absorption rate of electromagnetic radiation energy by a dielectric layer of thickness a per unit surface is [29]

$$\overline{Q}_1 = -a\overline{\boldsymbol{P}\dot{\boldsymbol{E}}_0}, \tag{8}$$

where $\boldsymbol{P} = -e\overline{n}_{\rm e}\xi(t)$ is the dipole moment per unit volume. By using (6–8), we obtain the relationship between the energy absorption rate and the damping constant in a one-dimensional system:

$$\Gamma_1 = \frac{4\pi\overline{Q}_1}{a\mathcal{E}_z^2}\frac{\omega^2}{\omega_{\rm p1}^2}. \tag{9}$$

For the spherically symmetric systems, calculations are analogous (see also [18]). In this case, the relationship between the damping constant and the energy absorbed in a unit time by the cluster has the form

$$\Gamma_3 = \frac{\overline{Q}_3}{a^3\mathcal{E}_0^2}\frac{\omega^2}{\omega_{\rm p3}^2}. \tag{10}$$

Thus, by using (9) and (10) and the calculated linear absorption rate $\overline{Q}$, we can find the damping constant Γ, which determines, in particular, the width of a surface plasmon. Below, the collisionless energy absorption rate and the corresponding damping constant are denoted by the small letters $\overline{q}$ and γ, while the rate $\overline{Q}$ and the constant Γ take into account all possible absorption mechanisms.

3. General expression for the absorption rate

A nanoplasma heated to temperatures of tens of electron-volts and over is a purely classical system (in particular, nondegenerate). Nevertheless, the simplest method of calculating the linear absorption rate is based on the quantum-mechanical perturbation theory. Of course, the final result does not contain Planck's constant.

In the self-consisted field approximation, the nanoplasma can be described in terms of N electrons occupying one-particle levels in a potential well. The interaction with the wave field induces electron transitions between the one-particle levels, with photon absorption or emission. The field energy absorbed by plasma in a unit time is proportional to the difference between the numbers of absorbed and emitted photons multiplied by the photon energy:

$$\overline{q} = N\hbar\omega\sum_{\boldsymbol{n},\boldsymbol{k}}\rho(\epsilon_{\boldsymbol{n}})(w^-_{\boldsymbol{nk}} - w^+_{\boldsymbol{nk}}), \tag{11}$$

where $w^-_{\boldsymbol{nk}}$ and $w^+_{\boldsymbol{nk}}$ are the electron-transition probabilities between the levels with quantum numbers $\boldsymbol{n}$ and $\boldsymbol{k}$, accompanied, respectively, by the absorption or emission of one photon with frequency ω. The index $\boldsymbol{n}$ denotes the full set of quantum numbers for the level; e.g., $\boldsymbol{n} \equiv \{n_{\rm r}, l, m\}$ for the spherical cluster, where $n_{\rm r}$, l, and m are the radial, orbital, and magnetic quantum numbers, respectively. Clearly, the absorption per unit surface is meaningful for the film. The quantum electron-energy distribution function $\rho(\epsilon_{\boldsymbol{n}})$ is normalised to unity. Considering that $w^+_{\boldsymbol{nk}} = w^-_{\boldsymbol{kn}}$ [see (14)], we obtain from (11)

$$\overline{q} = N\hbar\omega\sum_{\boldsymbol{n},\boldsymbol{k}}\left[\rho(\epsilon_{\boldsymbol{n}}) - \rho(\epsilon_{\boldsymbol{k}})\right]w^-_{\boldsymbol{nk}}. \tag{12}$$

Consider the simplest case of a one-dimensional system, where $\boldsymbol{n}$ is characterised by a single principal quantum number n (thin film homogeneous in the transverse direction). The electric field strength inside the film is given by expression (7). The electron–field interaction operator is

$$\hat{V}_{\rm int}(\boldsymbol{r}, t) = -e\boldsymbol{\mathcal{E}}(t)\boldsymbol{r}$$

$$= -e\mathcal{E}(t)(x\cos\chi + y\cos\theta\sin\chi + z\sin\theta\sin\chi). \tag{13}$$

The angles χ and θ are shown in Fig. 1. To the first order of the perturbation theory,

$$w^{\pm}_{nk} = \frac{\pi e^2\mathcal{E}_0^2}{2\hbar}\left|\langle k|z|n\rangle\right|^2\delta(\epsilon_k - \epsilon_n \pm \hbar\omega)\sin^2\theta\sin^2\chi. \tag{14}$$

According to the selection rules for electric dipole transitions, $k - n = 2s + 1$, $s = 0, \pm1, \pm2, \ldots$. In the limit $n,\ k \gg 1$, the quantum numbers and the quantum distribution function $\rho(\epsilon_n)$ can be expressed through the classical quantities according to the Bohr–Sommerfeld theory,

$$\sum_n \to \int {\rm d}n = \int\frac{{\rm d}\epsilon}{\hbar\Omega(\epsilon)}, \qquad \epsilon_k - \epsilon_n = \hbar\Omega(\epsilon_n)(2s+1),$$

$$\rho(\epsilon) = \hbar\Omega(\epsilon)f_1(\epsilon), \tag{15}$$

where $\Omega(\epsilon) = \hbar^{-1}{\rm d}\epsilon/{\rm d}n = 2\pi/T(\epsilon)$ is the frequency of electron oscillation with energy ϵ in the unperturbed self-consistent potential $U(z)$; $f_1(\epsilon)$ is the classical electron distribution function normalised as $\int {\rm d}\epsilon\, f_1(\epsilon) = 1$. This function is assumed to not be necessarily equilibrium. For this reason, by the temperature $T_{\rm e}$ below is meant the mean electron energy. The matrix element in (14) can be replaced by the Fourier component of the corresponding classical quantity [30]:

$$\langle k|z|n\rangle \to z_s(\epsilon) = \frac{\Omega(\epsilon)}{2\pi}\int_0^{T(\epsilon)} z(\epsilon, t)\exp[{\rm i}(2s+1)\Omega(\epsilon)t]{\rm d}t, \tag{16}$$

where $z(\epsilon, t)$ is the classical trajectory of an electron with energy ϵ. By using (14)-(16) and taking into account that the typical electron energies are far greater than the photon energy, i.e., $T_{\rm e} \gg \hbar\omega$, we obtain from (9) and (12) [17]

$$\gamma_1(\omega) = -\frac{\pi m_{\rm e}}{2}\omega^3\sum_s |z_s(\epsilon_s)|^2\left|\frac{\partial\Omega(\epsilon)}{\partial\epsilon}\right|^{-1}\left|_{\epsilon=\epsilon_s}\frac{\rm d}{{\rm d}\epsilon}\left[f_1(\epsilon)\Omega(\epsilon)\right]\right|_{\epsilon=\epsilon_s}. \tag{17}$$

Here, the summation is performed over all roots of the equation

$$(2s+1)\Omega(\epsilon_s) = \omega. \tag{18}$$

The meaning of condition (18) is clear: the nonzero contribution to the absorbed energy comes from only

those electrons whose oscillation period in the well with potential $U(z)$ is equal to the odd number of laser periods. Therefore, as in the case of waves in an infinite plasma, only resonance particles absorb, so that condition (1) is the analog of expression (1) for the finite system with size smaller than the radiation wavelength. In the absence of collisions, there is no reason for the phase interruption upon electron motion in the self-consistent potential, the contributions from many periods to the work of laser field are coherent, which provides a basis for condition (18). Any decoherence mechanism, including pair collisions, scattering from local-field fluctuations, and diffuse boundary conditions, renders absorption possible also for the particles with energies lying in a vicinity of the resonance energy ϵ_s.

In the case of three-dimensional geometry (spherical cluster), the calculations are similar to those presented above. The distinctions amount to the inclusion of angular motion. The corresponding computational details are given in Appendix 1. For the spherical cluster, the damping constant is expressed by

$$\gamma_3(\omega) = -\frac{\pi m_e \omega^3}{12} \sum_s \int_{M_{\min}}^{M_{\max}} M\,\mathrm{d}M \left\{ \frac{\mathcal{R}^+(\epsilon, M)}{s\Omega(\epsilon, M)} \left| \frac{\partial \Upsilon_+(\epsilon, M)}{\partial \epsilon} \right|^{-1} \times \left(\omega \frac{\partial}{\partial \epsilon} + \frac{\partial}{\partial M} \right) \left[\Omega(\epsilon, M) f_3(\epsilon, M) \right] \Big|_{\epsilon=\epsilon_s^+} + \frac{\mathcal{R}^-(\epsilon, M)}{s\Omega(\epsilon, M)} \left| \frac{\partial \Upsilon_-(\epsilon, M)}{\partial \epsilon} \right|^{-1} \left(\omega \frac{\partial}{\partial \epsilon} - \frac{\partial}{\partial M} \right) \times \left[\Omega(\epsilon, M) f_3(\epsilon, M) \right] \Big|_{\epsilon=\epsilon_s^-} \right\}. \tag{19}$$

Here, the classical energy and angular-momentum distribution function is related to the quantum distribution function $\rho(\epsilon_{n_r}, l)$ by the expression

$$f_3(\epsilon, M) = \frac{2\rho(\epsilon_{n_r}, l)}{\hbar^3 \Omega(\epsilon, M)}. \tag{20}$$

The functions $\mathcal{R}^{\pm}(\epsilon, M)$ are defined by

$$\mathcal{R}^{\pm}(\epsilon, M) = \left| \frac{\Omega(\epsilon)}{\pi} \int_0^{T/2} r(\epsilon, M, t) \cos[\omega t \pm \phi(\epsilon, M, t)] \mathrm{d}t \right|^2, \tag{21}$$

where $r(\epsilon, M, t)$ and $\phi(\epsilon, M, t)$ are the time-dependent radial coordinate and the azimuthal angle of a classical particle with energy ϵ and angular momentum M. The functions $\Upsilon_{\pm}(\epsilon, M)$ have the form

$$\Upsilon_{\pm}(\epsilon, M) = \Omega(\epsilon, M) \left(1 \pm \frac{\Delta\phi}{2\pi s} \right). \tag{22}$$

Here, $\Omega(\epsilon, M) = 2\pi / T(\epsilon, M)$ is the frequency of electron radial oscillations in the self-consistent potential $U(r)$, and

$$\Delta\phi = \left(\frac{2}{m_e} \right)^{1/2} M \int_{r_{\min}}^{r_{\max}} \frac{\mathrm{d}r}{r^2 \left[\epsilon - U(r) - M^2/(2m_e r^2) \right]^{1/2}}$$

is the increment in the azimuthal angle per period*. The sum in (19) goes over all roots $\epsilon_s^{\pm}(M)$ of the equation

$$s\Upsilon_{\pm}(\epsilon_s^{\pm}) = \omega, \tag{23}$$

which generalises (18) to the case of a spherically symmetric three-dimensional system.

Note that the sum over $s = n_r - n_r'$ in Eqn (19) [as also the corresponding sum in (17)] cannot be represented in the form of integral even in the classical limit. The latter is possible only if the separation between the neighboring resonance levels [solutions to Eqns (18) and (23)] is smaller than the mean electron energy and its dispersion in the well. For the self-consistent potential in the form of an infinitely deep rectangular well, the resonance levels become close to each other in the low-temperature limit $T_e \ll m_e \omega^2 a^2$ (Appendix 2). This situation is considered in detail in [17, 18].

Expressions (17) and (19) are the main results of this work. They can be used to estimate the rate of linear absorption of the intense laser radiation in a nanoplasma. Despite the fact that the system under consideration is purely classical and the absorption rate does not involve Planck's constant, the method of calculation based on the quantum-mechanical perturbation theory proved to be the simplest*. The same results can be obtained directly by the classical mechanics methods, but this involves more cumbersome calculations, particularly for $D \neq 1$.

4. Discussion

The expressions obtained above can be used to calculate the rate of linear collisionless absorption of laser radiation in a hot nanoplasma, provided that the form of the electron-trapping self-consistent potential and the distribution function are known. The determination of these quantities is a separate problem that requires numerical solution of the kinetic equation, which is beyond the scope of this work. We consider below the qualitative features of the collisionless absorption in a finite-size classical plasma using the simple model expressions for the self-consistent potential and the distribution function.

In Appendix 1, the damping constant $\gamma(\omega)$ is calculated for the one- and two-dimensional infinitely deep rectangular wells and for the field created by a charged infinite plane ('triangular' potential). The latter situation corresponds to the ionised homogeneous thin film in the case that electrons reside, for the most part, beyond the ion core. The electron velocity distribution is assumed to be Maxwellian with temperature T_e. The results of calculations are shown in Figs 2 and 3. For the one-dimensional rectangular well, the result exactly coincides with that obtained in [13]. One can see that dependence of the damping constant on the dimensionless variable (for the rectangular well) is virtually the same for the systems of different dimensionality. The dependence on the form of the self-consistent potential is of particular interest. In the rectangular well, $\gamma \sim T_e^{-3/2}$ at high temperatures, $T_e \gg T_0 = m_e(\omega a)^2$, and $\gamma \sim T_e^{1/2}$ at $T_e \ll T_0$. In the field of a charged layer (Fig. 3), the damping constant decreases at high temperatures somewhat slower: $\gamma \sim T_e^{-3/2} \ln T_e$, and it is exponentially small at low temperatures: $\gamma \sim \exp[-\pi^2/(8y^2)]$, where $y = \omega_0 (m_e T_e)^{1/2} a / U_0$ (see

*For a three-dimensional harmonic oscillator and Coulomb field, $\Delta\phi = 2\pi$, and expression (19) is greatly simplified. However, the self-consistent field in a heated cluster is obviously different from the fields in these simplest cases, so that there is no reason to discuss them in this work.

*The situation considered in this work is no exception. For instance, the dielectric constant of a high-temperature classical magnetised plasma was calculated in [31] also using the quantum-mechanical perturbation theory.

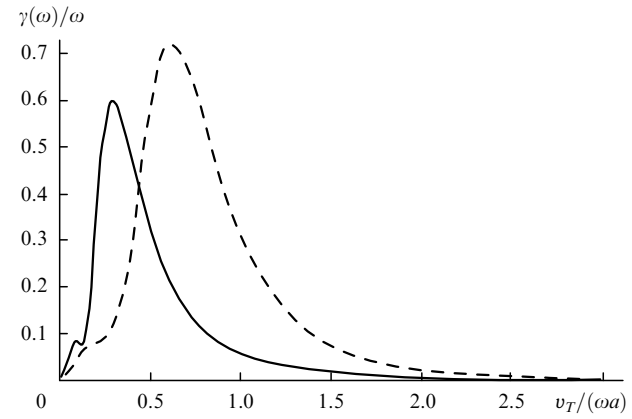

Figure 2. Damping constants for one-dimensional (solid line) and three-dimensional (dashed line) systems with a self-consistent potential simulated by a deep rectangular well.

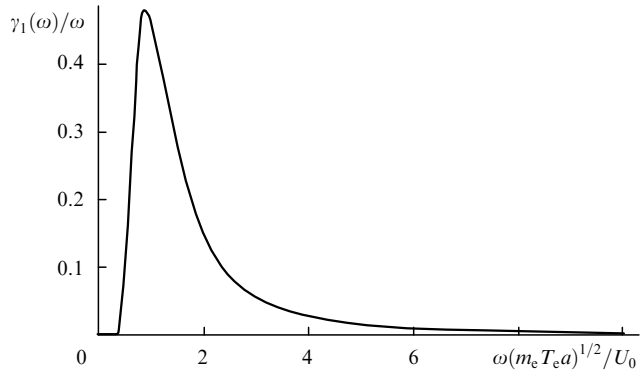

Figure 3. Damping constant for the one-dimensional system in the field of a charged plane.

Appendix 2). Such a distinction can easily be understood: the energy absorption is determined by the contribution from the resonance levels, while their positions are determined by the level density in the well, i.e., by the function $\Omega(\epsilon)$. In the rectangular well, the energy spectrum becomes sparse with increasing energy, whereas, in the triangular well, this happens with a decrease in energy. For this reason, the damping constant in the triangular well decreases exponentially in the low-temperature limit, when the distribution function is localised near the bottom of the well. In the infinite plasma, the behavior of the Landau damping constant is similar, provided that the condition $\omega \gg k_B v_T$ is fulfilled, where k_B is the Boltzmann constant and v_T is the electron thermal velocity [12].

In the low-temperature limit $v_T/(\omega a) \ll 1$, electron absorbs in a single collision with the wall the energy of the order of its ponderomotive energy in the internal laser field. This result is well known [13]. Interestingly, this result is obtained only for a deep rectangular well. One can see from the results obtained in Appendix 2 that the behavior of the damping constant in the field of a charged plane is quite different even in the high-frequency limit.

We now consider the dependence of the absorption rate on the form of the electron distribution function. The electron thermalisation in nanoplasma is controlled by the electron–electron collision frequency,

$$\nu_{ee} = \frac{4\sqrt{2\pi}}{3}\frac{e^4 \overline{n}_e L_C}{m_e^{1/2} T_e^{3/2}}, \tag{24}$$

where L_C is the Coulomb logarithm. For $\overline{n}_e \simeq 10^{22}$ cm^{-3} and $T_e \simeq 1$ keV, one has the estimate $\nu_{ee} \sim 10^{13}$ s^{-1}, which indicates that the thermalisation time can be comparable to the laser pulse duration. It follows that, by changing the pulse and target parameters, one can obtain nanoplasma with both Maxwellian and nonequlibrium electron distributions. Note that, upon transition to a nonequilibrium distribution with a small dispersion, the damping constant becomes more sensitive to the form of the resonance condition. One can see in Fig. 4 that, with a decrease in the distribution width, peaks arise on the curve $\gamma(\omega)$. Similar structures were observed in the analysis of the collisionless absorption in cold finite systems with the Fermi distribution [32]. The absorption peaks are clearly seen if the energy distribution is narrow: $\Delta \lesssim \delta\epsilon_s = |\epsilon_{s+1} - \epsilon_s|$, where Δ is the distribution width. The positions of the maxima of $\gamma_1(\omega)$ in the rectangular well are $\bar{\epsilon} = m_e(\omega a)^2/2$, $\bar{\epsilon} = 9m_e(\omega a)^2/2$, $\bar{\epsilon} = 25m_e(\omega a)^2/2$ ..., which coincide with ϵ_s in Eqn (18) for $s = 0, 1, 2, \ldots$. Here, $\bar{\epsilon}$ is the electron mean energy corresponding to the given distribution. The first resonance is seen even for the Maxwellian distribution (Fig. 2).

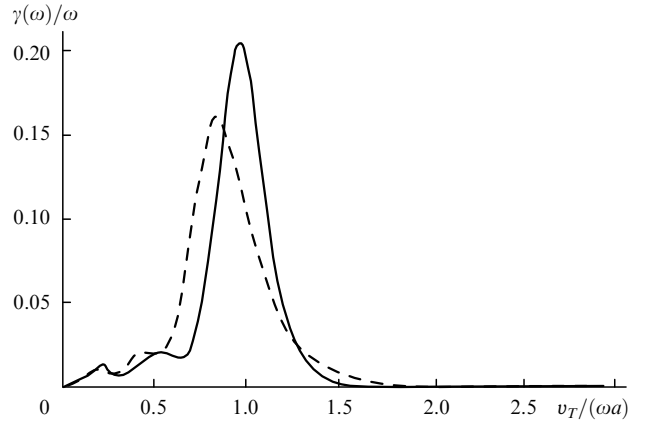

Figure 4. The damping constants for various electron distribution functions. One-dimensional system with infinitely deep rectangular potential is taken as an example. The functions $\rho(\epsilon) \sim \exp(-2\epsilon/T_e)$ (dashed line) and $\rho(\epsilon) \sim \exp(-10\epsilon/T_e)$ (solid line) were used as model distribution functions.

5. Conclusions

At least two effects considered in this work can be observed in the experimental studies of the interaction of intense laser pulses with the thin-film and cluster targets. First, the collisionless absorption of laser radiation can serve as an efficient mechanism of plasma heating. Let us show that this is possible under the conditions typical of the present-day experiments. The interaction of 10-nm clusters with pulses of intensity $I \simeq 10^{16}$ W cm^{-2} results in the primary (internal) atomic ionisation and formation of a nanoplasma with the mean electron energy of 200–300 eV. In obtaining this estimate, one should take into account that the typical drift energy of a photoelectron ionised by a linearly polarised laser field is $\bar{\epsilon}_{dr} \approx (E_0/E_a)U_p$, where E_a is the characteristic atomic-field strength and $U_p = e^2E_0^2/(4m_e\omega^2)$ is the electron ponderomotive energy in a linearly polarised

field with amplitude E_0 [33]. Using expressions (A2.17) and (10) and setting $\overline{n}_e = 10^{23}$ cm^{-3} and $\tau \simeq 100$ fs for the pulse duration, one obtains the following estimate for the mean energy absorbed by one electron during the pulse:

$$\Delta\epsilon \simeq \frac{\overline{q}\tau}{N} \simeq 10^3 \text{ eV}. \tag{25}$$

For a 10-nm thick film irradiated with a femtosecond pulse of intensity $I \simeq 10^{15}$ W cm^{-2}, the analogous estimate using expressions (A2.4) and (9) yields $\Delta\epsilon \simeq 10^2$ eV. Both estimates are in qualitative agreement with the experiment and the results of numerical simulation [4, 5]. For the above-mentioned parameters, the ratio $v_T/(\omega a) \ll 1$, because the damping constant is derived from the linear portion of the curves in Fig. 2*.

Second, the constant $\gamma(\omega)$ gives an estimate for the contribution of the collisionless damping mechanism to the width of the plasma resonance (the Mie resonance). By using the relation between $\overline{q}$ and γ [see (10)], we obtain with the above-mentioned parameters of laser pulse and cluster:

$$\hbar\gamma \simeq 0.4 \text{ eV}. \tag{26}$$

This estimate agrees well with the width of the linear Mie resonance; it can be obtained by the numerical simulation of cluster evolution in an intense laser field [34]. Thus, we can conclude that the collisionless absorption mechanism makes an appreciable, if not the main contribution to the heating rate of electron nanoplasma and to the width of surface plasmon for the nanosystems of size 10 nm and smaller irradiated by the femtosecond pulses with intensities $I \simeq 10^{14} - 10^{16}$ W cm^{-2}.

Nevertheless, the above estimates can be considered as an indirect evidence of the crucial role of the collisionless damping in hot plasma. The question now arises of the possibility of a direct experimental observation of this effect. The following possibilities are noteworthy. First, the collisionless damping in a homogeneous thin film arises only upon the excitation of plasma oscillations in the direction perpendicular to the film plane. As a result, the collisionless absorption rate becomes proportional to $\sin^2\theta \sin^2\chi$ [see (13) and Fig. 1] for an arbitrary orientation of the wave polarisation about the film surface; i.e., the absorption associated with the finite size of the film is possible only for the p-polarised wave component. Since the mean energy of electrons arisen from the film irradiation is proportional to the absorbed laser energy, this energy is expected to depend on the polarisation degree of the radiation. Moreover, because the various secondary processes in a nanoplasma (formation of multicharged ions, X-rays and UV radiation) arise mostly due to hot electrons, the efficiency of these processes is expected to depend on the polarisation of the incident radiation. Such dependences were observed in [4], where it was found that the X-radiation output for the p-polarised wave is several times greater than for the s-polarised wave. Repetition of the experiment [4] with the aim of analysing these dependences can provide a quantitative estimate for the collisionless damping effect.

Second, to observe the damping effect, its dependence on the nanobody size can be used. Indeed, if the condition $v_T \ll \omega a$ is fulfilled (which is easily realised for thin films and clusters; see estimates above), the rate of energy absorption by an electron changes in inverse proportion to the body size, irrespective of its dimensionality. For this reason, the collisionless energy absorption mechanism becomes inefficient for the systems of size 100 nm and over. The dependence of the mean electron energy on the film thickness was observed in [4] upon the film irradiation by the femtosecond pulses with intensity $I \simeq 10^{15}$ W cm^{-2}. The dependence of the absorption rate on the system size can be observed by irradiating the oriented nonspherical nanotargets with femtosecond pulses and measuring the dependence of electron mean energy in the spectrum on the target orientation.

Finally, the width of surface plasmon can be measured as a function of the parameters of laser pump pulse in the pump-probe experiment. The pump pulse produces nanoplasma in a thin film or cluster, while the weak probe pulse of several tens of femtoseconds in duration is scattered by nanoplasma with a controlled delay after the pump pulse. By varying the delay time, one can control the value of ω_{pD} at the instant of interaction, to achieve linear resonance and measure its width. The parameters of the pump pulse determine the properties of nanoplasma and, in particular, its electron temperature. Thus, one can determine the temperature dependence of the plasmon width and compare it with the results of calculations by expressions (17) and (19).

Note that these results are mostly qualitative. This is caused by the fact that many factors governing the nanoplasma dynamics in the field of an intense electromagnetic radiation cannot be taken into account within the framework of a simple analytic model. A more thorough study of the collisionless absorption of laser radiation in nanoplasma can be carried out only on the basis of numerical simulation with allowing for the realistic form of the self-consistent potential, the distribution function, the nonstationary character of interaction (ion-core expansion, electron evaporation from the system), and the contribution from the nonlinear processes. The model formulas obtained in this work can be used for the numerical estimates and qualitative analysis of the results of numerical simulation.

Acknowledgements. We are grateful to W. Becker and S.V. Fomichev for useful discussions and to B.M. Karnakov and S.P. Goreslavskii for valuable remarks. This work was supported by the Russian Foundation for Basic Research (Grant No. 06-02-16916a), the Deutsche Forschungsgemeinschaft (Grant No. DFG 436 RUS 113/852/0-1), the President Program for Support of the Leading Scientific Schools (Grant No. NSh-320.2006.2), and the Ministry of Education and Science of the Russian Federation (Grant RNP No. 2.1.1.1972).

Appendix 1. Derivation of expression (19)

For a spherically symmetric system (cluster), the energy absorption rate (12) is given by the expression

$$\overline{q} = \frac{\pi e^2 \mathcal{E}_0^2 \omega}{2} N \sum_{n_r,l,m} \sum_{n'_r,l',m'} |\langle n_r l m | r\cos\theta | n'_r l' m' \rangle|^2 \times \left[\rho(\epsilon) - \rho(\epsilon')\right] \delta(\epsilon - \epsilon' - \hbar\omega). \tag{A1.1}$$

*For $a = 10$ nm, $\omega = 1.55$ eV, and $T_e \approx 10$ eV, $v_T/(\omega a) \approx 0.1$.

The level energies $\epsilon(n_r, l)$ depend on the radial (n_r) and azimuthal (l) quantum numbers; the interaction operator has the form $\hat{V} = -e\boldsymbol{\mathcal{E}}_0 \boldsymbol{r}\cos(\omega t)$; and the quantisation axis is chosen along the direction of field polarisation.

Using the properties of 3j-symbols [30], one can calculate the sum over magnetic quantum numbers in (A1.1):

$$\sum_{m,m'} |\langle lm|\cos\theta|l'm'\rangle|^2 = \frac{l+1}{3}\delta_{l\,l'-1} + \frac{l}{3}\delta_{l\,l'+1}$$

$$\approx \frac{l}{3}\left(\delta_{l\,l'-1} + \delta_{l'\,l'+1}\right). \qquad \text{(A1.2)}$$

Next, by using the standard quasi-classical representation of the radial wave functions, one obtains for the radial matrix element [35] the following expression:

$$\langle n_r, l\,|r|n_r', l\pm 1\rangle$$

$$= \frac{\Omega(\epsilon, M)}{\pi}\int_0^{\pi/\Omega} r(t)\cos[\omega t \pm \phi(\epsilon, M, t)]\mathrm{d}t, \qquad \text{(A1.3)}$$

where $M = \hbar l$ is the classical angular momentum; $\Omega(\epsilon, M) = \hbar^{-1}(\partial\epsilon/\partial n_r)_l$ is the frequency of radial oscillations of a particle in the self-consistent potential $U(r)$; and $\phi(\epsilon, M, t)$ is the azimuthal rotation angle of the trajectory. Expression (21) is obtained from (A1.3).

Let us go from the summation over the radial quantum numbers n_r, n_r' in (A1.1) to the summation over n_r and $s = n_r - n_r'$. In the classical limit, the levels are closely spaced, so that the sum over n_r can be replaced by the integral over energy and calculated using the relation

$$\delta(\epsilon - \epsilon' + \hbar\omega)$$

$$= \hbar^{-1}\delta\left[\Omega(\epsilon, M)(n_r - n_r') + \frac{1}{\hbar}\left(\frac{\partial\epsilon}{\partial l}\right)_{n_r}(l - l') + \omega\right]. \qquad \text{(A1.4)}$$

As a result, we obtain expressions (19–23).

Appendix 2. Damping constant for model potentials

Let us obtain the damping constant $\gamma(\omega)$ for the simplest potentials using (17) and (19) and assuming the Gibbs' electron distribution with temperature T_e in the well: $\rho(\epsilon) = Z^{-1}(T_e)\exp(-\epsilon/T_e)$. In this case,

$$f_1(\epsilon) = \frac{\exp(-\epsilon/T_e)}{\Omega(\epsilon)Z_1(T_e)},\quad Z_1(T) = \int\frac{\mathrm{d}\epsilon}{\Omega(\epsilon)}\exp(-\epsilon/T_e),$$

$$f_3(\epsilon, M) = \frac{\exp(-\epsilon/T_e)}{\Omega(\epsilon, M)Z_3(T_e)}, \qquad \text{(A2.1)}$$

$$Z_3(T) = \int\mathrm{d}\epsilon\int M\mathrm{d}M\frac{\exp(-\epsilon/T_e)}{\Omega(\epsilon, M)}.$$

One-dimensional rectangular well. In the case of a one-dimensional infinitely deep rectangular well of width a one has

$$\Omega(\epsilon) = \frac{\pi}{a}\left(\frac{2\epsilon}{m_e}\right)^{1/2}$$

and the solutions of (18) take the form

$$\epsilon_s = \frac{m_e\omega^2 a^2}{2\pi^2(2s+1)^2}.$$

Expressions for the matrix elements (16) and the normalisation constant for the distribution function in (A2.1) are, respectively,

$$|z_s(\epsilon)|^2 = \frac{8\epsilon}{\pi^2 m_e\omega^2},\ Z_1(T_e) = a\left(\frac{m_e T_e}{2\pi}\right)^{1/2}, \qquad \text{(A2.2)}$$

so that expression (17) gives

$$\gamma_1 = \frac{64}{\pi^6 x^3}\omega\sum_{s=0}^{\infty}\frac{\exp\left\{-4/\left[\pi^3(2s+1)^2x^2\right]\right\}}{(2s+1)^5},$$

$$x = \left(\frac{8T_e}{\pi m_e\omega\, 2a^2}\right)^{1/2} \equiv \frac{v_T}{\omega a}. \qquad \text{(A2.3)}$$

This formula follows also from the expression for the imaginary part of the dielectric constant of a homogeneous plasma layer [13]. The limit $x \ll 1$ corresponds to cold plasma in a relatively wide well, so that the sum in (A2.3) can be replaced by integral. As a result, we obtain

$$\gamma_1 \approx \omega x. \qquad \text{(A2.4)}$$

This limiting case corresponds to the linear portion of the curves in Fig. 2. In the opposite high-temperature limit, the exponential factor in (A2.2) can be set equal to unity. Then

$$\gamma_1 \approx 0.13\frac{\omega}{x^3}. \qquad \text{(A2.5)}$$

Field of a charged plane. In the case when the self-consistent field is created by a charged infinite plane (triangular well), we have

$$U(z) = U_0\left|\frac{z}{a}\right|. \qquad \text{(A2.6)}$$

In this case,

$$\Omega(\epsilon) = \frac{\pi U_0}{2a}\frac{1}{(2m_e\epsilon)^{1/2}}$$

and the expression for the roots of Eqn (18) takes the form

$$\epsilon_s = \frac{\pi^2 U_0^2(2s+1)^2}{8m_e\omega^2 a^2}.$$

Then

$$|z_s(\epsilon)|^2 = \frac{32\epsilon}{\pi^4(2s+1)^4 m_e\omega^2},$$

$$Z_1(T_e) = \frac{a}{\pi U_0}\left(2\pi m_e T_e^3\right)^{1/2}. \qquad \text{(A2.7)}$$

Substitution of these expressions into (17) gives

$$\gamma_1(\omega) = 2\left(\frac{2}{\pi}\right)^{1/2}\frac{\omega}{y^3}\sum_{s=0}^{\infty}\frac{\exp\left[-\pi^2(2s+1)^2/(8y^2)\right]}{2s+1},$$

$$y = \frac{\omega(m_e T_e)^{1/2}a}{U_0}. \qquad \text{(A2.8)}$$

As in the case of rectangular well, the damping constant is a function of one variable. The function $\gamma_1(y)/\omega$ is shown in Fig. 3. In the limiting cases of large and small y, expression (A2.8) is simplified:

$$\gamma_1 \approx 2\left(\frac{2}{\pi}\right)^{1/2}\frac{\omega}{y^3}\exp\left(-\frac{\pi^2}{8y^2}\right), \quad y \ll 1, \qquad \text{(A2.9)}$$

$$\gamma_1 \approx \left(\frac{2}{\pi}\right)^{1/2}\frac{\omega}{y^3}\ln\left(\frac{\sqrt{8}y}{\pi}\right), \qquad y \gg 1. \qquad \text{(A2.10)}$$

The first of these expressions corresponds to cold plasma in a deep well, and the second, to high temperatures.

Spherical well. In the case when the self-consistent cluster potential is simulated by an infinitely deep spherical well

$$U(r) = \begin{cases} 0, & r \leqslant a, \\ \infty, & r > a, \end{cases}$$

it is convenient to pass to new variables in (19)–(23)

$$\mu \equiv \arctan\left(\frac{a^2}{b^2}-1\right)^{1/2}, \ \zeta \equiv \frac{M\omega}{2\epsilon}\left(\frac{a^2}{b^2}-1\right)^{1/2},$$

$$b = \left(\frac{M^2}{2m_e\epsilon}\right)^{1/2},$$

where a is the cluster radius. By using these variables, we obtain

$$\Omega(\mu,\zeta) = \frac{\pi\omega}{\zeta}, \qquad \text{(A2.11)}$$

$$\mathcal{R}^{\pm}(\mu,\zeta) = \frac{b^2}{\zeta^2}\cos^2\mu\left[\left(1 \pm \frac{\tan\mu}{\zeta}\right)\sin\zeta \mp \tan\mu\cos\zeta\right]^2, \qquad \text{(A2.12)}$$

$$\Upsilon_{\pm}(\mu,\zeta) = \frac{\pi\omega}{\zeta}\left(1 \pm \frac{1}{j}\frac{\mu}{\pi}\right), \qquad \text{(A2.13)}$$

where j is an integer. Equation (23) takes the form

$$\zeta = \pm\mu + \pi j. \qquad \text{(A2.14)}$$

The normalisation constant for the distribution function in (A2.1) is

$$Z_3(T_e) = \frac{(2m_e T_e a^2)^{3/2}}{6\sqrt{\pi}}. \qquad \text{(A2.15)}$$

Substituting expressions (A2.11)–(A2.15) into (19), one obtains

$$\gamma_3 = \frac{64\omega}{\pi^2 x^5}\int_0^{\pi/2} d\mu \sin^9\mu\cos\mu\left\{\sum_{j=0}^{\infty}\exp\left[-\frac{4\sin^2\mu}{\pi x^2(\pi j+\mu)^2}\right]\right.$$

$$\left.\times\frac{1}{(\pi j+\mu)^7} + \sum_{j=1}^{\infty}\exp\left[-\frac{4\sin^2\mu}{\pi x^2(\pi j-\mu)^2}\right]\frac{1}{(\pi j-\mu)^7}\right\}. \qquad \text{(A2.16)}$$

The dependence of this function on the dimensionless variable x is illustrated in Fig. 2. In the low-temperature limit, the sums in (A2.16) can be replaced by integrals, whereupon the following expression is obtained for the damping constant [18]:

$$\gamma_3 = \frac{1}{2}\omega x. \qquad \text{(A2.17)}$$

References

1. Smirnov B.M. *Usp. Fiz. Nauk*, **170**, 495 (2000).
2. Calvayrac F., Reinhard P.-G., Suraud E., Ullrich C.A. *Phys. Rep.*, **337**, 493 (2000).
3. Krainov V.P., Smirnov M.B. *Phys. Rep.*, **370**, 237 (2002).
4. Volkov R.V., Gordienko V.M., Dzhidzhoev M.S., Zhukov M.A., Mikheev P.M., Savel'ev A.B., Shashkov A.A. *Kvantovaya Electron.*, **24**, 1114 (1997) [*Quantum Electron.*, **27**, 1081 (1997)].
5. Ditmire T., Donnelly T., Rubenchik A.M., Falcone R., Perry M.D. *Phys. Rev. A*, **53**, 3379 (1996).
6. Zweiback J., Ditmire T., Perry M.D. *Opt. Express*, **6**, 236 (2000).
7. Santra R., Greene C.H. *Phys. Rev. Lett.*, **91**, 233401 (2003).
8. Taguchi T., Antonsen Th.M. Jr, Milchberg H.M. *Phys. Rev. Lett.*, **92**, 205003 (2004).
9. Krainov V.P., Rastunkov V.S. *Laser Phys.*, **15**, 262 (2005).
10. Kostyukov I.Yu. *Zh. Eksp. Teor. Fiz.*, **127** (5), 1026 (2005).
11. Landau L.D. *Zh. Eksp. Teor. Fiz.*, **16** (7), 574 (1946).
12. Lifshits E.M., Pitaevskii L.P. *Physical Kinetics* (Oxford: Pergamon Press, 1981; Moscow: Nauka, 1979).
13. Gil'denburg V.B. *Zh. Eksp. Teor. Fiz.*, **43** (4), 1394 (1962).
14. Kawabata A., Kubo R. *J. Phys. Soc. Jpn*, **21**, 1765 (1966).
15. Kostyukov I.Yu. *Pis'ma Zh. Eksp. Teor. Fiz.*, **73** (8), 438 (2001).
16. Megi F. et al. *J. Phys. B: At. Mol. Opt. Phys.*, **36**, 273 (2003).
17. Zaretsky D.F., Korneev Ph.A., Popruzhenko S.V., Becker W. *J. Phys. B: At. Mol. Opt. Phys.*, **37**, 4817 (2004).
18. Korneev Ph.A., Popruzhenko S.V., Zaretsky D.F., Becker W. *Laser Phys. Lett.*, **2**, 452 (2005).
19. Bystrov A.M., Gil'denburg V.B. *Zh. Eksp. Teor. Fiz.*, **127** (2), 478 (2005).
20. Mulser P., Kanapathipillai M. *Phys. Rev. A*, **71**, 063201 (2005).
21. Mulser P., Kanapathipillai M., Hoffmann D.H.H. *Phys. Rev. Lett.*, **95**, 103401 (2005).
22. Kundu M., Bauer D. *Phys. Rev. Lett.*, **96**, 123401 (2006).
23. Last I., Jortner J. *Phys. Rev. A*, **64**, 063201 (2001).
24. Fomichev S.V., Popruzhenko S.V., Zaretsky D.F., Becker W. *J. Phys. B: At. Mol. Opt. Phys.*, **36**, 3817 (2003).
25. Ginzburg V.L. *The Propagation of Electromagnetic Waves in Plasmas* (Oxford: Pergamon Press, 1971; Moscow: Nauka, 1967).
26. Jasapara J. et al. *Phys. Rev. B*, **63**, 045117 (2001).

27. Wabnitz H. et al. *Nature*, **420**, 482 (2002).
28. Laarmann T. et al. *Phys. Rev. Lett.*, **92**, 143401 (2004).
29. Landau L.D., Lifshits E.M. *Electrodynamics of Continuous Media* (Oxford: Pergamon Press, 1984; Moscow: Nauka, 1982).
30. Landau L.D., Lifshits E.M. *Quantum Mechanics* (Oxford: Pergamon Press, 1977; Moscow: Nauka, 1989).
31. Galitskii V.M., Migdal A.B., in *Fizika plazmy i problema upravlyaemykh termoyadernykh reaktsii* (Plasma Physics and the Problem of Controlled Thermonuclear Reactions), Ed. by M.A. Leontovich (Moscow: Akad. Nauk SSSR, 1958) Vol. 1, p. 161.
32. Santer M., Mehlig B. *Physica E*, **11**, 8 (2001).
33. Popov V.S. *Usp. Fiz. Nauk*, **174**, 921 (2004).
34. Fomichev S.V., Zaretsky D.F., Becker W. *J. Phys. B: At. Mol. Opt. Phys.*, **37**, L175 (2004).
35. Berson I.Ya. *Zh. Eksp Teor. Fiz.*, **83** (4), 1276 (1982).